

## Research Article

# Preparation and Characterization of TiO<sub>2</sub> Nanostructure by TiCl<sub>4</sub> Hydrolysis with Additive NaOH

Rashed Taleb Rasheed

Department of Applied Sciences, Chemistry Division, University of Technology, IRAQ

Correspondent Author Email: [r\\_awsy@yahoo.com](mailto:r_awsy@yahoo.com)

### Article Info

Received  
08/09/2016

Accepted  
21/05/2017

### Abstract

Titanium dioxide (TiO<sub>2</sub>) nanostructures were synthesized via the hydrolysis of TiCl<sub>4</sub> in alcohol / water solution/with sodium hydroxide solution in the ice-bath (0-5 °C). The particles were characterized by using X-ray diffraction technique (XRD), spectroscopy of Ultra Violet-Visible (UV / Visible) and infrared (FT-IR), atomic force microscope (AFM) and scanning electron microscope (SEM) analysis were used in order to gain information about the material, morphology, size and the shape of the particles.

**Keywords:** TiO<sub>2</sub> nanostructures, TiCl<sub>4</sub>, hydrolysis.

### الخلاصة

تم تحضير ثنائي اوكسيد التيتانيوم (TiO<sub>2</sub>) بواسطة التحلل لرابع كلوريد التيتانيوم (TiCl<sub>4</sub>) في محلول مائي/كحولي مع محلول هيدروكسيد الصوديوم في حمام ثلجي (0-5 °C). تم تشخيص الراسب المتكون باستخدام تقنية حيود الاشعة السينية (XRD)، مطيافية الاشعة فوق البنفسجية / المرئية (Uv/Visible) والاشعة تحت الحمراء (FT-IR)، ومجهر القوى الذرية (AFM) لدراسة الاطوار والحجم الحبيبي للجسيمات النانوية وتم دراسة طوبوغرافية السطح باستخدام المجهر الالكتروني الماسح (SEM).

## Introduction

Titanium dioxide (TiO<sub>2</sub>) or titania, is one of the most attracted materials in nanotechnology and nanoscience because of a very useful semiconducting transition and exhibits unique characteristics such as non-toxicity, easy handling and low cost [1]. Interests towards the nanostructures titanium dioxide (TiO<sub>2</sub>) was grown in the past decades, due to its interesting physical and chemical properties [2] [3].

These advantages make TiO<sub>2</sub> a material in solar cells, fuel cell, environmental purification applications, a pigment, selfcleaning, surfaces, resistance to photochemical, chemical erosion and chemical sensors for hydrogen gas evolution [1] [4] [5]. Titania has three different crystalline phases: brookite (orthorhombic), anatase [6] and rutile [7]. Rutile is the most stable phase at sizes greater than 35 nm, while brookite is more stable than anatase for crystal sizes greater than 11 nm. Among these phases, the TiO<sub>2</sub> exists mostly as anatase and rutile which have the tetragonal structures while brookite has orthorhombic structure [8].

However, the high-temperature stable phase is rutile [9].

Several methods have been reported in the literature to prepare TiO<sub>2</sub>, including the hydrolysis of titanium alkoxides, acidic solutions of Ti (IV) salts, oxidations of TiCl<sub>4</sub> on gaseous phase [10], sputtering, chemical vapor deposition and sol-gel process [11]. Among them, one of the most used methods is the sol-gel technique due to its excellent chemical homogeneity and possibility of deriving unique metastable structure at low reaction temperatures [12]. The different routes were usually found produced different results. Even for the same route, the obtained powder size is different when using a different amount of the starting materials [13]. Many methods have been employed to prepare TiO<sub>2</sub> films, including sol-gel process, chemical vapor deposition, e-beam evaporation and sputtering.

The sol-gel conventional method uses the hydrolytic route, which involves the initial hydrolysis of the chloride or alkoxide precursor followed by continual condensations between the hydrolyzed particles forming the gel [14]. In this work, we

have prepared TiO<sub>2</sub> nanostructures using TiCl<sub>4</sub> as a precursor.

## Materials and Methods

Titanium tetrachloride (TiCl<sub>4</sub>), sodium hydroxide (NaOH) and ethanol (EtOH) absolute grade, all these chemicals have purity 99.9%, where obtained from Fluka Company in high purity and no further purification was done before use.

### Synthesis of TiO<sub>2</sub> nanostructures

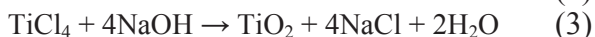
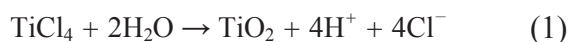
TiO<sub>2</sub> nanostructures were prepared by sol-gel technique using titanium tetrachloride (TiCl<sub>4</sub>), absolute ethanol (EtOH), distilled water, and sodium hydroxide (NaOH) as the starting materials. TiCl<sub>4</sub> is added to a mixture of water/ alcohol (50:50) in an ice bath.

The receiving water is maintained at 0°C while TiCl<sub>4</sub> is added dropwise under vigorous stirring. The resulting precursor solution has a TiCl<sub>4</sub>:H<sub>2</sub>O volume ratio of 1:40 and pH ≈ 1. Subsequent condensation of the hydrolysis product results in gel formation.

In order to obtain a more stable suspension, the Cl<sup>-</sup> concentration was reduced and pH increased to around 2.5 by added dropwise of sodium hydroxide solution under vigorous stirring and the gel is precipitated from the suspension. The resulting material is then subjected to repeated cycles of centrifugation, washing, and resuspension until the final product, usually in powder form, is considered free from impurities.

## Results and Discussion

We prepared crystalline titanium dioxide by sol-gel precipitation method using titanium tetrachloride in aqueous solution and subsequently annealed at 300°C and 500 °C. As soon as TiCl<sub>4</sub> hydrolyses TiO<sub>2</sub> particles, H<sup>+</sup> and Cl<sup>-</sup> ions were generated, the process of reaction can be described by the following steps [15]:



The general process for preparing TiO<sub>2</sub> by sol-gel process, at low temperature, anatase is the primary structure phase formed observed which transforms only upon annealing to rutile phase which is thermodynamically more condense and most stable [16]. As annealing treatment prolonged the

rutile XRD peaks became sharper indicating the formation of larger r-TiO<sub>2</sub>.

### Calcinations temperature

#### Characterization of Nanostructures

The XRD is employed for the identification and understanding the crystalline growth nature of titanium dioxide structures prepared by sol-gel method. Calcination is a common treatment used to improve the crystallinity of TiO<sub>2</sub> powders [12]. Two phase structures of titanium dioxide powders were characterized at (300 and 500 °C) for (4-hours), by X-ray diffraction (XRD) at room temperature.

Major peaks corresponding to the tetragonal TiO<sub>2</sub> were observed.

The diffraction peak at 2θ with 27.5°, 36.2°, 39.2°, 41.3°, 44.1°, 54.4°, 56.6°, 62.6°, 64.1°, 68.8°, and 70.0° corresponds to the (110), (101), (200), (111), (210), (211), (220), (002), (310), (301) and (112) planes of rutile TiO<sub>2</sub> (JCPDS Card No.21-1276), respectively, except the peaks (2θ = 64.1° and 70.0°) corresponds to the crystal planes of (310) and (112) respectively, were undistinguished at 300 °C calcination, indicating the formation of rutile phase of TiO<sub>2</sub>. Our FT-IR peaks are in good agreement with the literature report [17]. The presence of titanium dioxide particles was confirmed by the location of the peaks which compared to literature values [18]. As a result of annealing, the nanostructures are found to have increased intensity and a slight reduction of the full width at half maximum (FWHM). The crystalline size of the titanium dioxide calculated by the equation of Debye-Scherrer's which is given by:

$$D = K\lambda / (\beta \cos\theta) \quad (4)$$

Where *D* is the crystal size; *K* is usually taken as 0.89, *β* is the line width at half-maximum height (FWHM) and *λ* is the wavelength of the X-ray radiation (*λ*=0.15406 nm) for CuKα [19]. The representative XRD charts, Figure 1, samples as-prepared and calcined at (300 and 500 °C).

Miller indices provided in the Figure 1 and all peaks determine the transformation of calcined powder to TiO<sub>2</sub> crystallites with tetragonal rutile crystal structure. In addition, the increasing of the calcination temperature causes increases the number of reflection. We can calculate the lattice

constant of the titanium dioxide particles by using the formula:

$$1/d^2 = ((h^2 + k^2)/a^2) + (l^2/c^2) \quad (5)$$

Where ( $d$ ) is the interplanar distance, ( $a$ ) and ( $c$ ) are the lattice constant for the tetragonal structure and ( $h k l$ ) are the Miller indices. The calculated crystalline size ( $D$ ) and lattice constant ( $a$  and  $c$ ) of  $TiO_2$  are tabulated in Table 2.

It is observed that the  $TiO_2$  crystallinity improves with increasing substrate temperature (300 °C to 500 °C) for study peaks (110, 101 and 211) evident from XRD pattern. The crystallite size of  $TiO_2$  obtained using Debye-Scherrer's equation and the XRD parameters of nanostructures at various crystalline orientations at 300 °C and 500 °C respectively were shown in Table 1.

#### Scanning Electron Microscope (SEM) Analysis

SEM was used to further examine the morphology, crystallinity, and shape and particle size of the sample. A SEM image of  $TiO_2$  nanostructures in rutile phase are shown in Figure 2. It is clearly seen that the  $TiO_2$  consist of shapes like porous hollow.

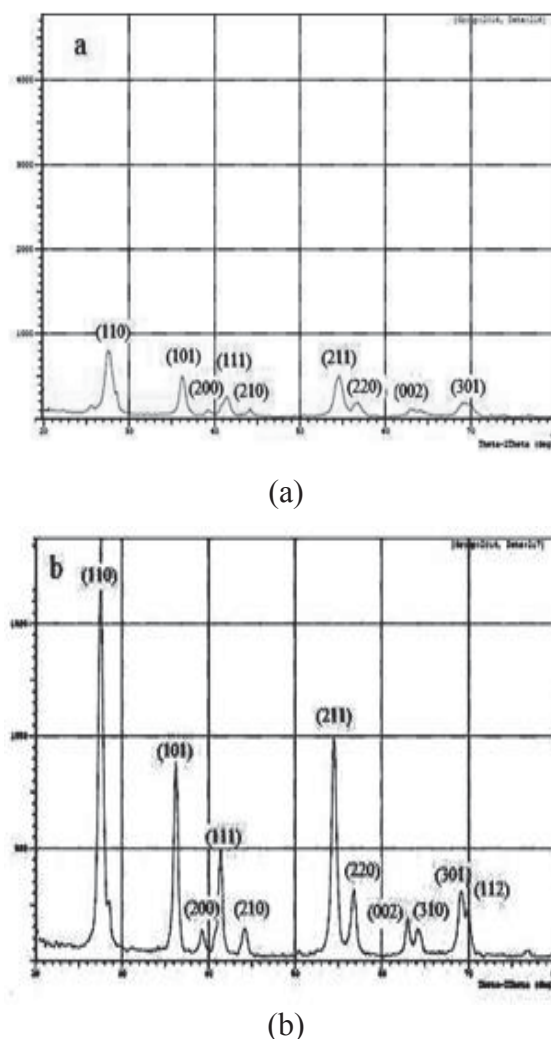


Figure 1: XRD peaks for the prepared  $TiO_2$  nanostructures after annealing at (a) 300 °C and (b) 500°C for (4 hours).

Table 2: The crystallite size and lattice parameters of  $TiO_2$  nanostructures.

| Substrate temperature | $hkl$ | $d(\text{Å})$ | $2\theta$ | $\theta$ | FWHM ( $\beta$ ) | $D(\text{Å})$ | $a(\text{Å})$ | $c(\text{Å})$ |
|-----------------------|-------|---------------|-----------|----------|------------------|---------------|---------------|---------------|
| 300 °C                | 110   | 3.226         | 27.560    | 13.833   | 1.029            | 7.955         | 4.562         | 4.271         |
|                       | 101   | 3.118         | 28.600    | 14.300   | 0.500            | 16.390        | -             | -             |
|                       | 211   | 1.682         | 54.502    | 27.250   | 1.140            | 7.835         | -             | -             |
| 500 °C                | 110   | 3.233         | 27.560    | 13.780   | 0.670            | 12.206        | 4.572         | 4.263         |
|                       | 101   | 3.118         | 28.600    | 14.300   | 0.431            | 19.014        | -             | -             |
|                       | 211   | 1.683         | 54.446    | 27.223   | 0.677            | 13.194        | -             | -             |

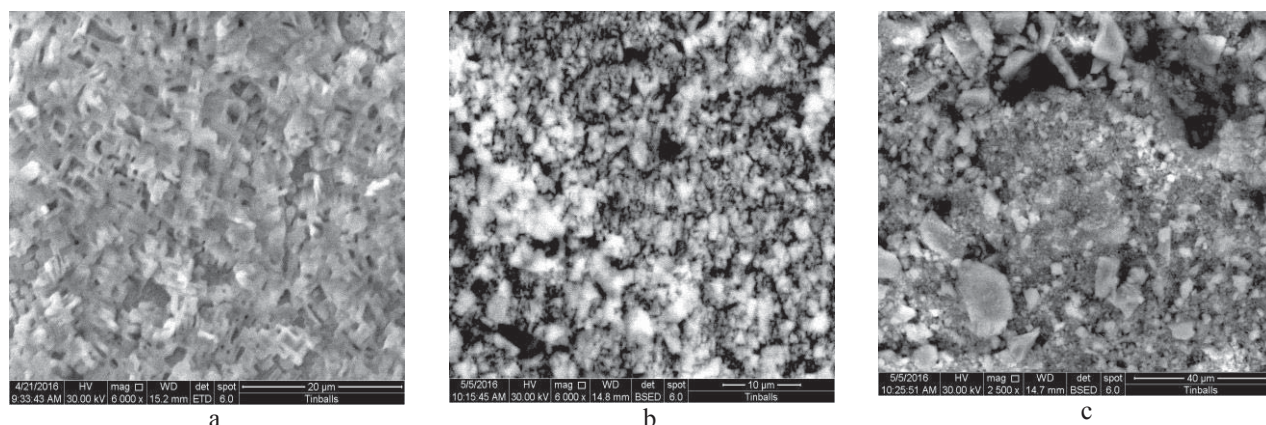


Figure 2: A top-view SEM image of TiO<sub>2</sub> nanostructures annealing at (a) 100 °C (b) 300 °C and (c) 500 °C for (4- hours).

### FT-IR Spectroscopy

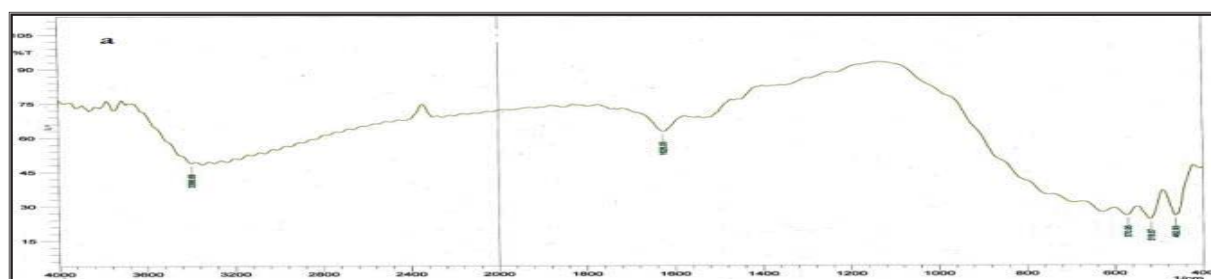
It is well known that the vibrational spectroscopy is a very useful technique for the determination of the functional groups of titanium dioxide nanostructures. The FT-IR spectrum of TiO<sub>2</sub> nanostructures shows in Figure 3. The peaks, in the spectra around, to 3400 and 1630 cm<sup>-1</sup> are due to stretching and bending vibration of the –OH group respectively. In the FT-IR spectra, all the peaks observed were around 560-460 cm<sup>-1</sup> represent to both stretching and bending of Ti-O-Ti group [4]. When annealing at (300 °C and 500 °C) the broad peaks of O-H stretching vibration become smaller with increase temperature and the Ti-O stretching become broad and more significant.

### Atomic force microscope (AFM)

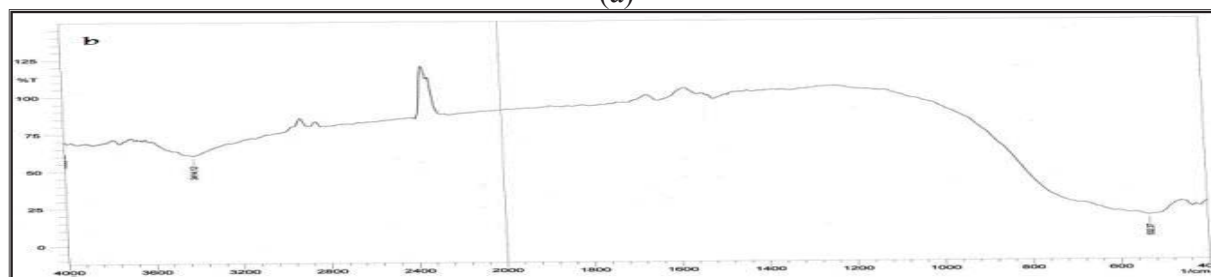
Figure 3 shows a typical three-dimensional atomic force microscope (AFM) images and the cor-

responding size distributions of the titanium dioxide nanostructures as prepared, annealing at 300 °C and 500 °C. As shown in the Figure the better surface quality and crystallographic structure are obtained.

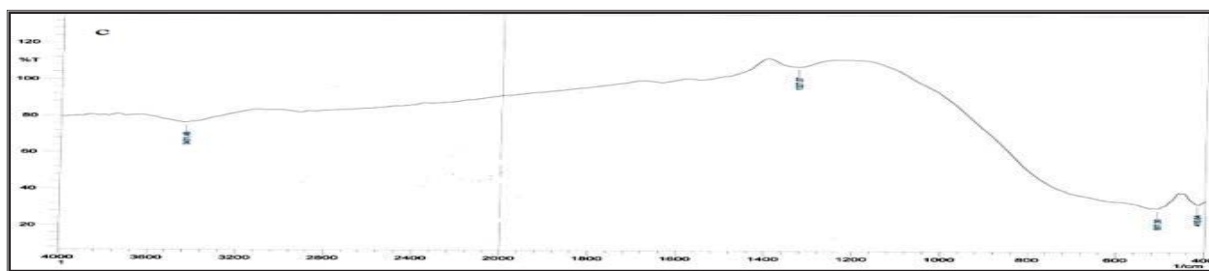
It's clear from the Figure 4 that TiO<sub>2</sub> nanostructures are porous in shape, having an average diameter of 64.56 nm, 94.29 nm and 100.48 nm for as-prepared, annealing at 300 °C and 500 °C respectively. The 3-dimensional (3D) AFM image of material nanostructures in which the regularly distributed TiO<sub>2</sub> nanostructures pillars and voids over the entire surface can be seen with a maximum value and morphology with a root-mean-square (RMS) roughness and average diameter as shown in Table 2.



(a)



(b)



(c)

Figure 3: FT-IR spectra of TiO<sub>2</sub> annealing at (a) 100 °C (b) 300 °C and (c) 500 °C for (4 hours).

Table 2: Roughness average, root-mean-square (nm) roughness and the average diameter of TiO<sub>2</sub> annealing at 100 °C, 300 °C and 500 °C in nm units.

| Samples | Roughness average | root-mean-square (RMS) roughness | Average Diameter |
|---------|-------------------|----------------------------------|------------------|
| 100 °C  | 0.612             | 0.712                            | 64.56            |
| 300 °C  | 0.335             | 0390                             | 94.29            |
| 500 °C  | 0.637             | 0.746                            | 100.48           |

ured by using UV-Vis spectrophotometer. The UV- Vis optical properties in the range (250–1000) nm at various temperatures (as-prepared (100), 300 and 500 °C) showed temperature dependent transmittance and absorbance, as shown in Figure 5. Both samples (300 and 500 °C) showed a slight decrease in optical transmittance at higher temperatures. This is probably due to the increased particle size and surface roughness, and also to the phase transformation from anatase to rutile which results in band gap decrease and led to higher surface scattering [20].

### Optical Properties

The optical transmittance and absorbance of the TiO<sub>2</sub> solution (0.001 M) in ethanol, was meas-

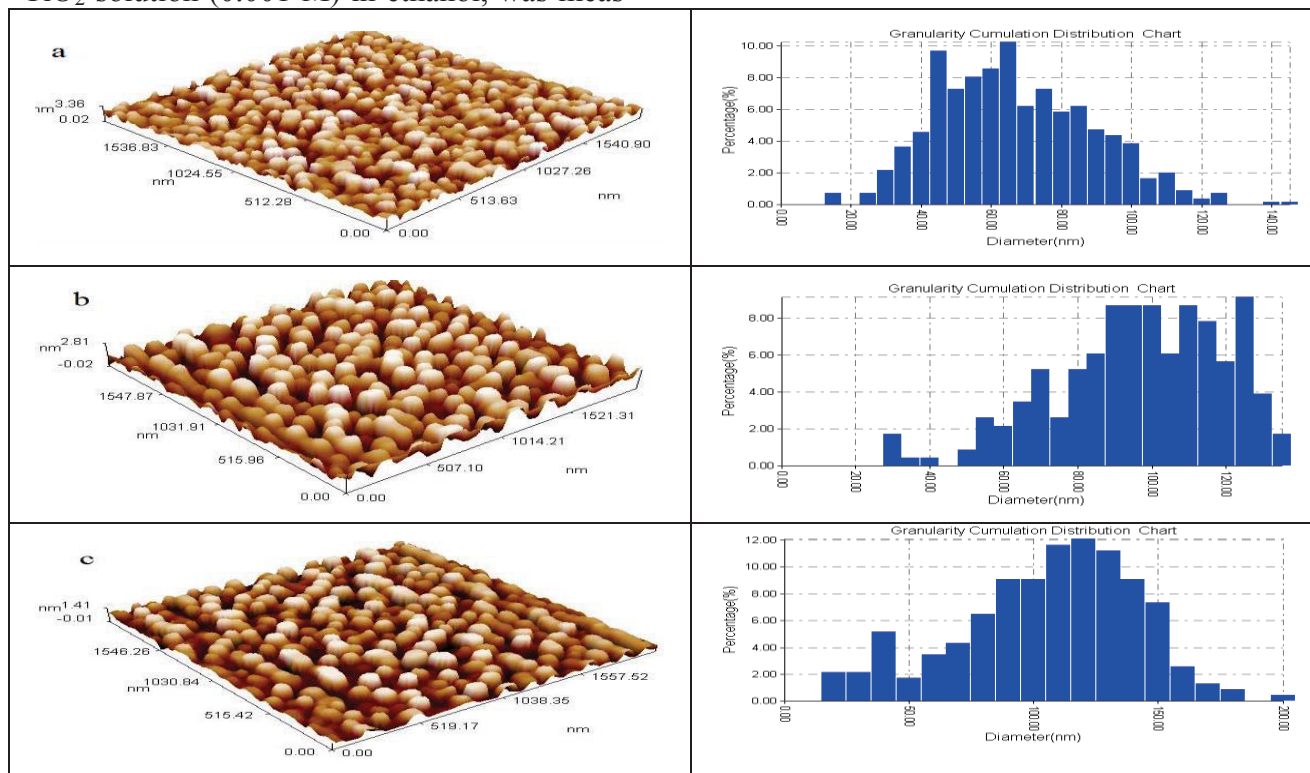


Figure 4: AFM image of TiO<sub>2</sub> nanostructures annealing at (a) 100 °C (b) 300 °C and (c) 500 °C.

The optical band gaps were measured by plotting  $(\alpha h\nu)^2$  versus  $h\nu$  for TiO<sub>2</sub> thin films prepared by dip coating technique are illustrated in Figure 6. The band gap values: (3.24, 3.19 and 3.21 eV) are corresponding to the (as-prepared, 300 and 500) °C. The optical band gaps were measured by plotting  $(\alpha h\nu)^2$  versus  $h\nu$  for TiO<sub>2</sub> films and are illustrated in Figure 6. The band gap energy ( $E_g$ ) of as-prepared TiO<sub>2</sub> nanoparticles (3.31 eV), which is larger than that values of (3.25 and 3.20 eV) for the bulk TiO<sub>2</sub>, corresponding to the (300 and 500) °C temperatures respectively.

This can be explained because the band gap of the semiconductors has been found to be particle size dependent [21]. The band gap decreases with increasing particle size and the absorption edge is shifted to a lower energy (red shift) with increasing particle size.

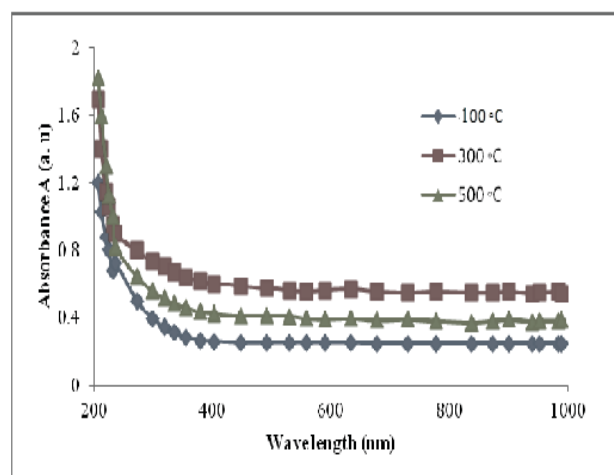
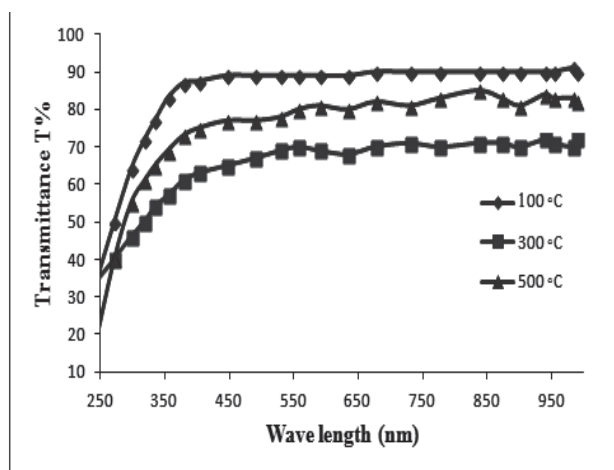


Figure 5: Optical Transmission (upper) and Absorption (lower) as a function of wavelength for TiO<sub>2</sub> at different temperatures (100, 300 and 500 °C).

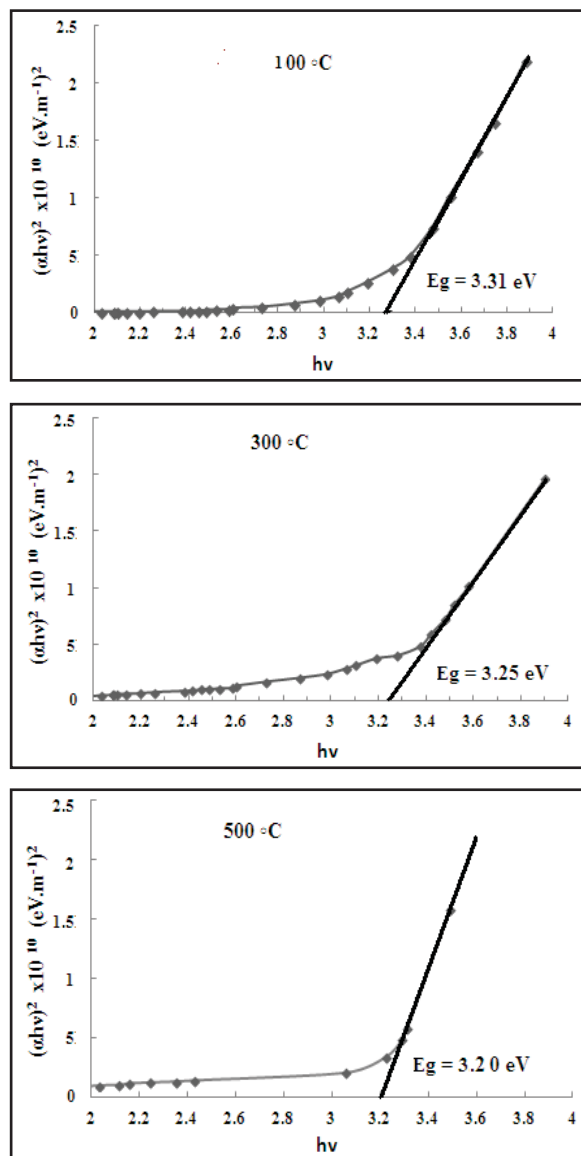


Figure 6: A plots of  $(\alpha h\nu)^2$  versus photon energy ( $h\nu$ ) of TiO<sub>2</sub> thin films with different temperature: 100 °C, 300 °C and 500 °C.

## Conclusions

TiO<sub>2</sub> nanoparticles have been prepared from titanium tetrachloride (TiCl<sub>4</sub>) with sodium hydroxide solution. We confirmed the nanoparticles by X-ray diffraction (XRD) and subsequently annealed at 300 and 500 °C. The studies of surface morphological obtain from SEM micrograph showed that the particles with the shapes like porous hollow are rutile in nature. Based on the XRD, SEM and AFM analyses, the current study shows that the size range of the nanoparticles is (64.56, 94.29 and 100.48 nm) at a temperature (As-prepared (100 °C), 300 °C and 500 °C) respectively.

## Acknowledgements

The author would like to thank the University of Technology, Applied Sciences Department for technical assistance to complete this work.

## References

- [1] S. M. W. C. a. D. B. M. R. Hoffmann, "Environmental Applications of Semiconductor Photocatalysis," *Chem. Rev.*, vol.95, no.1, pp.69-96, 1995.
- [2] A. P. K. Z. J. P. a. P. Y. S. A. Sher Shah, "Green synthesis of biphasic TiO<sub>2</sub>-reduced graphene oxide nanocomposites with highly enhanced photocatalytic activity," *ACS Appl. Mater. Interfaces*, vol.4, pp.3893-3901, 2012.
- [3] R. B. Z. a. L. Gao., "Synthesis of nanosized TiO<sub>2</sub> by hydrolysis of alkoxide titanium in micelles.," *Eng. Mate*, vol.573, pp.224-226, 2002.
- [4] R. V. a. R. S. R. Sharmila Devi, "Synthesis of Titanium Dioxide Nanoparticles by Sol-Gel Technique," *I. J. I. R. S. E. T.*, vol.3, no.8, pp.15206-15211, 2014.
- [5] D. O. A. C. -. G. a. S. J. -. S. N. Castillo, "Structural and morphological properties of TiO<sub>2</sub> thin films prepared by spray pyrolysis.," *Revista Mexicana De Física*, vol.50, no.4, p.382, 2004.
- [6] B. L. B. a. M. A. Anderson., "Peptization Process in the Sol-Gel Preparation of Porous Anatase (TiO<sub>2</sub>).," *Chem. Mater.*, vol.7, pp.1772-1778, 1995.
- [7] T. I. a. X. S. J. -G Li., "Anatase, brookite, and rutile nanocrystals via redox reactions conditions: phase-selective synthesis and physicochemical properties.," *J. Phys. Chem. C*, vol.111, pp.4969-4976, 2007.
- [8] M. -S. Z. J. -M. H. a. Z. Y. K. -R. Zhu, "Size effect on phase transition sequence of TiO<sub>2</sub> nanocrystal.," *Mater. Sci. Eng.*, vol.403, pp.87-93, 2003.
- [9] G. Brady, *Materials Handbook*, New York: McGraw-Hill., 1971.
- [10] C. L. A. C. Y. Z. a. D. F. L. Shi, "Morphology, and structure of nanosized TiO<sub>2</sub> particles synthesized by gas-phase reaction.," *Materials Chemistry and Physics*, vol.66, no.51(1), pp.51-57, 2000.
- [11] K. S. Mazdiyasi., "Powder synthesis from metal-organic precursors," *Ceram Int.*, vol.8, no.2, pp.42-45, 1982.
- [12] X. X. a. J. N. J. Zhang, "Hydrothermal hydrolysis synthesis and photocatalytic properties of nano-TiO<sub>2</sub> with an adjus table crystalline structure.," *Journal of Hazardous Materials*, vol.176, pp.617-622, 2010.
- [13] B. X. W. M. Y. a. L. L. Li, "Preparation and characterization of nano-TiO<sub>2</sub> Powder," *Mater. Chem. Phys*, vol.78, pp.184-188, 2002.
- [14] E. I. T. D. S. S. D. M. C. R. V. P. G. P. a. H. I. N. R C Suci., "TiO<sub>2</sub> thin films prepared by sol - gel method.," *Journal of Physics: Conference Series*, vol.182, pp.1-4, 2009.
- [15] D. W. B. a. M. R. H. C. Kormann, "Preparation and Characterization of Quantum-Size Titanium Dioxide.," *Journal of Physical Chemistry*, vol.92, pp.5196-5201, 1988.
- [16] B. -Y. H. a. C. -M. T. C. Su, "Sol-gel preparation and photocatalysis of titanium dioxide.," *Catalysis Today*, vol.96, no.3, pp.119-126, 2004.
- [17] P. L. a. B. N. K. Thamaphat, "Phase Characterization of TiO<sub>2</sub> Powder by XRD and TEM.," *Nat. Sci.*, vol.42, pp.357-361, 2008.
- [18] M. U. f. N. K. a. E. h. M. Akarsu, "A Novel Approach to the Hydrothermal Synthesis of anatase titania Nanoparticles and the Photocatalytic Degradation of Rhodamine B," *Turk J Chem*, vol.30, no.3, pp.333-343, 2006.
- [19] B. D. Cullity, *Elements of X-Ray Diffraction*, Addison-Wesley, 1978.
- [20] Y. A. A. H. A. J. a. Y. K. Z. K. Sarmad S, "Annealing Effect on the Growth of Nanostructured TiO<sub>2</sub> Thin Films by Pulsed Laser Deposition (PLD)," *Eng. and Tech. Journal*, vol.31B, no.4, pp.460-470, 2013.

- [21] S. M. A. R. K. Madhusudan Reddy, "Bandgap studies on anatase titanium dioxide nanoparticles. ," *Materials Chemistry and Physics.*, vol.78, pp.239-245, 2002.